Journal of Basic and Applied Engineering Research
p-ISSN: 2350-0077; e-ISSN: 2350-0255; Volume 3, Issue 13; October-December, 2016, pp. 1164-1168

http://www.krishisanskriti.org/Publication.html

Broadband Second Harmonic Generation in Mid Infrared Region in a Multi-tapered Zinc Telluride Slab using Total Internal Reflection Quasi Phase Matching

Bhaswati Medhi[1] and Sumita Deb[2]

[1,2]National Institute of Technology Agartala, Jirania, Tripura (West), Tripura, Pin – 799046, India
E-mail: [1]bhaswatimtech@gmail.com, [2]sumita_nita@rediffmail.com

Abstract—*We have analytically described the concept of broadband second harmonic generation (SHG) in mid-IR region in an isotropic multi-tapered semiconductor slab made of Zinc Telluride (ZnTe) semiconductor. A computer aided simulation has been carried out to obtain the second harmonic intensity when the slab is incident with a broadband fundamental laser radiation and the phenomenon of total internal reflection (TIR) takes place within the slab of 10 mm length. We have also considered the absorption losses, reflection losses and Goos-Hänchen (GH) shift in this process.*

1. INTRODUCTION

Broadband SHG has been the field of interest for so many applications like spectroscopy, amplification of fiber communication, optical coherence tomography, imaging, tuning of temperature, etc. In regard to potential needs of efficient SHG with usable broad bandwidth, quasi phase matching (QPM) has proven to be the most promising technique.

There has been considerable effort to enhance the bandwidth (BW) of SHG through QPM (a) by adopting special geometries like domain engineered nonlinear gratings [1] and Cerenkov phase matching [2], which are strictly wavelength dependent, and (b) by choosing specific material systems that exhibit zero group velocity mismatch around the phase matching wavelength for SHG [3,4]. However, it is often not possible to exploit the maximum non-linear coefficient of the crystal, leading to smaller conversion efficiencies [4]. In techniques involving periodic poling, fabrication errors from the ideal domain period lead to phase error accumulation between the interacting fields, which degrades the conversion efficiency.

The concept of QPM using TIR in a plane parallel slab was first suggested by Armstrong et al. [5], which has been subsequently demonstrated in an isotropic semiconductor (GaAs, ZnSe, ZnS) slab for resonant QPM SHG by Boyd and Patel [6] and by Komine et al. [7]. The same technique has been extended as non-resonant QPM toward Difference Frequency Generation (DFG) in isotropic semiconductor by Haidar et al. [8]. Baudrier – Raybaut et al. have shown in their paper [9] that efficient frequency conversion can be achieved in disordered polycrystalline isotropic materials by a random QPM technique. The frequency converted waves generated by the individual domains of the polycrystalline structure achieve random QPM technique. The frequency-converted waves those are generated by the individual domains of the polycrystalline structure acquire random phases and interfere neither constructively nor destructively and the output intensity is given as the sum of the intensities due to individual domains. This technique has been implemented in transparent (ZnSe) [9] and in opaque (GaP) [10] semiconductors. Ardhendu Saha and Sumita Deb have also implemented the concept of random QPM in near infrared (NIR) region for generation of broadband SH in a tapered structure semiconductor slab made of ZnSe [11].

The objective of this paper is to analytically demonstrate broadband SHG in a multi-tapered slab of an isotropic semiconductor made of ZnTe crystal, in the mid-IR region, using the TIR-QPM technique. Since a multi-tapered slab is considered, where there will be a converging section and a diverging section, the length between the successive bounces will decrease to the mid-point and then increase till the end of the slab (as shown in Fig. 1), as the incident beam propagates through the slab, thereby ensuring the possibility of non-resonant and resonant, as well as random QPM. With the help of simple geometry, the variation of proposed slab dimensions has been considered. The conversion efficiency and 3dB BW has been obtained with the help of computer aided simulation. Some of the factors like surface roughness, GH-shift and linear absorption have also been considered in this analysis.

2. PROPOSED SCHEME

For broadband SHG we have proposed a mono-crystalline multi-tapered isotropic semiconductor slab configuration of slab length L = 10 mm and thickness t = 400 μm as shown in Fig. 1. Here, t_1= 2 μm, t_2= 20 μm, t_3=15 μm, t_4=10 μm and L_2=L_3= L-L_Z where L_Z=1 mm. The upper surfaces GA and GB are tapered with angles θ_1 and θ_3 respectively with respect to their base nomenclature as RT. Similarly, the lower surfaces MD and MC are tapered with angles θ_2 and θ_4 with respect to their base PU respectively. The tapering angles are determined by the vertical heights i.e., t_1, t_2, t_3 and t_4 of the multi-tapered slab. The face where the beam of fundamental laser light has been made incident is cut at an angle ψ with respect to a plane perpendicular to the horizontal plane.

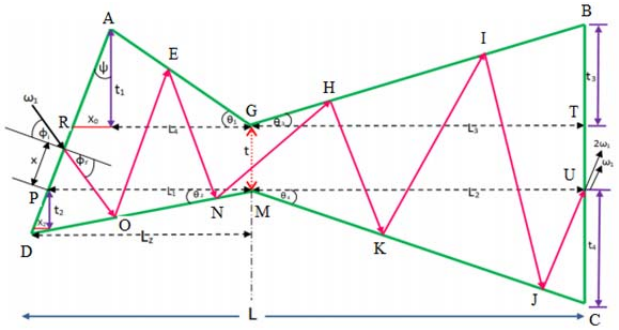

Fig. 1: Geometry of multi-tapered semiconductor slab

Let the fundamental broadband optical radiation having center frequency ω_1 be incident at an angle ϕ_i with respect to the normal to the inclined slab end face. The angle of incidence ϕ_1 on the horizontal plane inside the semiconductor slab will be determined by the refractive index of the material. If ϕ_1 is greater than the critical angle, for the range of input frequencies, then the collimated optical radiation will undergo TIR inside the multi-tapered slab. In our proposed structure, there are two parts – the first part is converging section and the second part is diverging section (as shown in Fig.1). Therefore, the angle of incidence and the successive interaction length will tend to decrease in the converging section and then gradually increase in the diverging section for this multi-tapered structure, thereby corresponding to non-resonant QPM since the interaction lengths between successive bounces cannot be optimized to be equal to an odd multiple of the coherence length L_{coh} ($=\frac{\pi}{\Delta k}$, where Δk is the dispersive wave vector mismatch) for all the frequencies available in the input band. However, a situation may coincide with an odd multiple of the coherence length of another frequency in the band, and so forth. The conversion efficiency for that particular frequency will be higher for that particular interaction length since it will then correspond to resonant QPM. However, the conversion efficiencies of other frequencies will be lower for that interaction length owing to non-resonant QPM. The phase shifts of the interacting waves indeed vary randomly during their propagation inside the slab, thereby giving rise to a situation identical to that of random QPM, wherein the constructive as well as the destructive interference effects of the interacting waves are destroyed. Clearly, the proposed scheme is less efficient than the truly phase-matched condition because the latter benefits from the constructive interference of the waves generated by different parts of the non-linear medium, but it outperforms the phase matched scenario for which the interference of the generated waves is destructive, thereby resulting in a flatter spectral BW.

2.1 Polarization

Based on the three interacting waves ω_1, ω_2 and ω_3 (where ω_1, ω_2 are the input wavelengths and ω_3 is the output wavelength) we have considered the ppp polarization configuration where 'p' denotes the orientation of the electric field parallel to the plane of incidence. The expression for d-coefficient for ppp polarization can be expressed as $d_{ppp} = 6d_{ij}\cos^2\phi_n \sin\phi_n \cos\tau \sin\tau$, with the slab being oriented along [001] direction, τ is the angle which the incidence-plane makes with [100] direction and ϕ_n is the generalized angle of incidence inside the slab, which is given by $\phi_n = (n-1)\theta + \phi_1$, where $\phi_1 = \frac{\pi}{2} - (\sin^{-1}\frac{\sin\phi_i}{n_1}) + \psi$ and n = 1, 2, 3, .. so on. Here d_{ij} is d_{14} since ZnTe belongs to symmetry class $\bar{4}3$ m and its value is considered to be 90 pm/V.

2.2. Factors limiting conversion yield

The SHG conversion yield is limited by three significant factors, namely the surface roughness, GH shift and absorption loss of the material.

2.2.1. Surface Roughness

When light is incident on a rough surface, it undergoes scattering at reflection, which in turn causes a drop in the amount of reflected light. This drop is measured in terms of Strehl Ratio [8]. In our case, a peak to valley value (p-v value) of the surface is considered to be 30 nm in the computer aided simulation.

2.2.2. Goos-Hänchen shift (GH-shift)

GH-shift depends on the wavelength of the incident radiation, which leads to reduction in the usable crystal length. This effect may be neglected in case of SHG since the two waves will undergo the same amount of longitudinal shift and the total GH shift encountered by the waves may be considered as negligible as compared to the total slab length. In our

proposed slab, the GH shift has been calculated for both upper and lower tapered surfaces in both converging as well as in the diverging section.

2.2.3. Absorption

Linear absorption can be very detrimental to the frequency conversion process and places severe limits on the conversion efficiency values. Usually, the linear absorption co-efficient α_ω is much less than 1. Generally, the absorption of the fundamental cannot be eliminated, although at very low absorption it is often masked by scattering. For SHG, at values of $\alpha_{2\omega} l \geq 5$ (where l is the interaction length) the phase matching curve changes shape from sinc^2 to Lorentzian. Absorption has another demerit on heating of the material. Since the refractive indices and wave vector mismatch ΔK are functions of temperature, absorption can produce a drift in the phase matching conditions and a reduction in conversion efficiency. In our case, we have considered a linear absorption coefficient ($\alpha_\omega \approx \alpha_{2\omega}$) of 0.0008 cm^{-1} for the selected material.

3. RESULT AND DISCUSSION

Computer aided simulation has been done to obtain the conversion efficiency and 3db bandwidth considering input beam intensity $I_\omega \approx 10$ MW/cm^2, input fundamental broadband source of (7-19) μm. The slab dimensions are set as L = 10 mm and the vertical heights of the multi-tapered slab as t = 400 μm, t_1 = 9 μm, t_2 = 20 μm, t_3 = 15 μm and t_4 = 10 μm. The input conditions at the entry point are chosen as $\phi_i = 0.9$ radian and $x = 190$ μm. The angle ϕ_i is chosen in such a way that all the wavelengths present in the input band satisfy the condition of TIR inside the slab. For the analysis, the temperature is chosen to be 300 K. From the simulation results, it can be observed that, when the reflection loss, absorption loss and GH shift is considered the efficiency comes out to be 4.687 % and the 3db bandwidth as 8419.24 nm. The analytical results thus obtained indicate the possibility of an extremely high spectral bandwidth. Since efficiency is low when losses are considered, therefore the spectral bandwidth is very broad. The reason behind this drop in efficiency can be explained by the effect of surface roughness on the generated intensity of each wavelength as the fundamental optical beam travels through the slab.

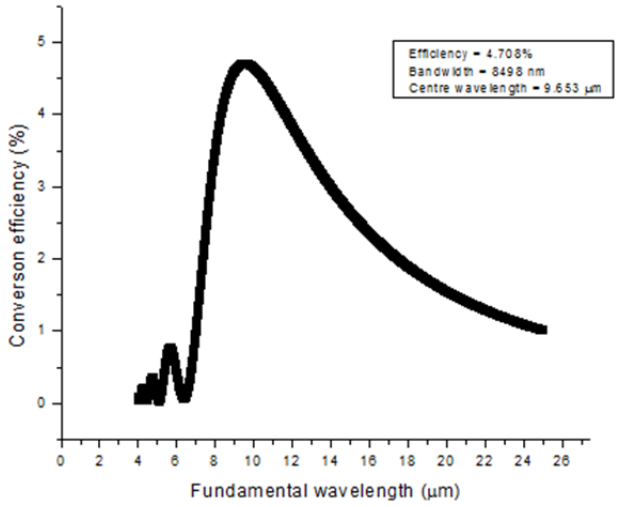

Fig. 2: Plot of conversion efficiency vs input wavelength for the multi-tapered ZnTe slab considering all the losses (scattering, absorption, GH shift)

3.1 Effect of variation in tapering angles

Table 1: Variation in conversion efficiency and bandwidth with change in tapering angle

Thickness (t) (μm)	Peak conversion efficiency (%)	3db BW (nm)	Centre wavelength (μm)
400	4.687	8339.80	9.5923
450	4.888	8578.09	9.9283
500	5.170	8895.80	10.3010
550	5.319	9292.91	10.5820

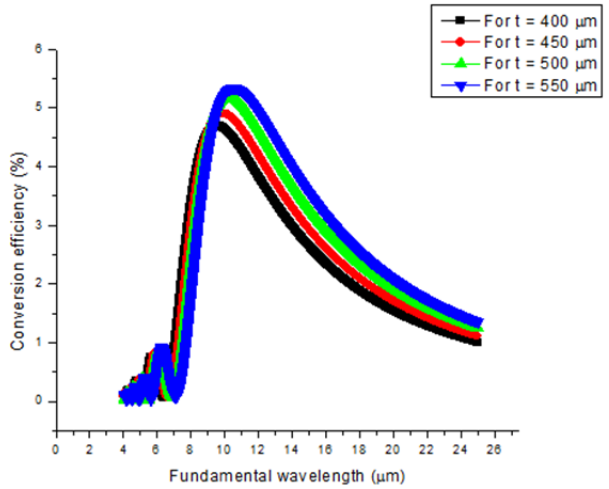

Fig. 3: Plots of conversion efficiencies and bandwidths with variation of tapering angles

3.2 Variation in the vertical heights of the slab

Table 3: Variation in conversion efficiency and bandwidth with variation in vertical height t_1 of the slab

Vertical height t_1 (μm)	Peak conversion efficiency (%)	3db wavelength (nm)	Centre wavelength (μm)
5	4.532	8419.24	9.653
7	4.718	8498.67	9.592
11	4.829	8498.67	9.592

Table 4: Variation in conversion efficiency and bandwidth with variation in vertical height t_2 of the slab

Vertical height t_2 (μm)	Peak conversion efficiency (%)	3db wavelength (nm)	Centre wavelength (μm)
10	4.341	8626.97	9.708
15	4.526	8498.59	9.653
20	4.670	8419.20	9.592

Table 5: Variation in conversion efficiency and bandwidth with variation in vertical height t_3 of the slab

Vertical height t_3 (μm)	Peak conversion efficiency (%)	3db wavelength (nm)	Centre wavelength (μm)
5	4.751	8419.24	9.531
10	4.798	8419.24	9.592
15	4.687	8419.24	9.592

Table 6. Variation in conversion efficiency and bandwidth with variation in vertical height t_4 of the slab

Vertical height t_4 (μm)	Peak conversion efficiency (%)	3db wavelength (nm)	Centre wavelength (μm)
5	4.814	8339.81	9.592
10	4.687	8419.24	9.592
15	4.734	8419.24	9.653

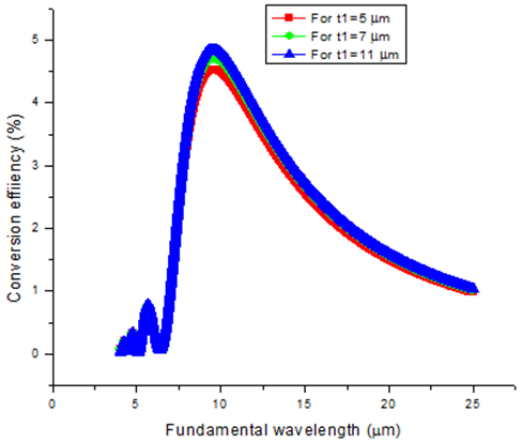

(a)

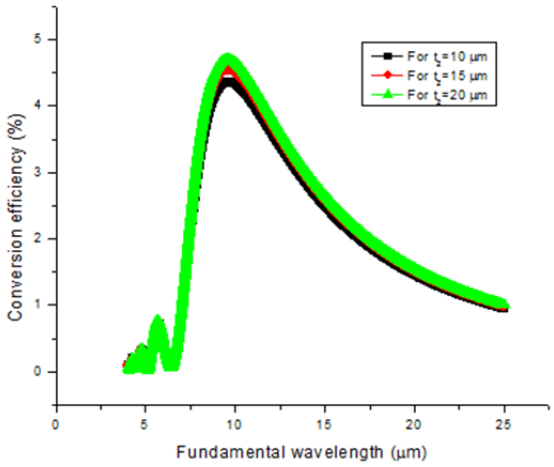

(b)

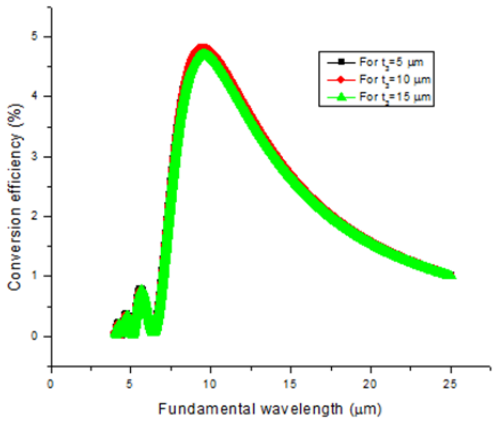

(c)

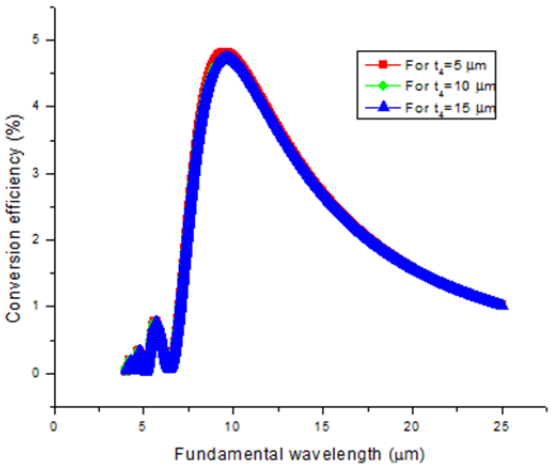

(d)

Fig. 7: Plots of conversion efficiencies and bandwidths with variation of vertical heights (a) t_1, (b) t_2, (c) t_3, (d) t_4

4. CONCLUSION

In this paper, a broadband frequency converter based on a multi-tapered slab made of isotropic semiconductor Zinc Telluride (ZnTe) has been analyzed numerically. The converter provides an extremely wide 3db bandwidth of 8419.24 nm, centered at 9.653 □m, in the mid infrared region. It can be considered as a simple yet competitive means of obtaining extremely wide broadband SHG.

REFERENCES

[1] Ashihara, S., Shimura, T., and Kuroda, K., "Group velocity matched second harmonic generation in tilted quasi pase matched gratings", Journal of Optical Society America B, 20,1, May 2003, pp. 853-856.

[2] Wang, G.Y., and Garmire, E.M., "High efficiency generation of ultrashort second harmonic pulses based on the Cerenkov geometry", Opt. Letters, 19, 15, February 1994, pp. 254-256.

[3] Yu, N.E., Ro, J.H., Cha, M., Kurimura, S., and Taira, T., "Broadband Quasi-Phase-Matched Second Harmonic Generation in MgO-Doped Periodically Poled $LiNbO_3$ at the Communications Band", Optics Letters, 27, 2002, pp. 1046-1048.

[4] Zhu, H., Wang, T., Zheng, W., Yuan, P., Qian, L., and Fan, D., "Efficient second harmonic generation of femtosecond laser at one micron", Optics Express, 12, 17, May 2004, pp. 2150-2155.

[5] Armstrong, J.A., Bloembergen, N., Ducuing, J., and Pershan, P.S., "Interactions between Light Waves in a Nonlinear Dielectric", Physical Review, 127, 15, September 1962, pp.1918.

[6] Boyd, G.D., Patel, C.K.N., "Enhancement of optical harmonic generation by reflection phase matching in ZnS and Ga As ", Appl. Phys. Letts., 8, 1966, pp. 313.

[7] Komine, H., W.H. Long, Jr., Tully, J.W. and Stappaerts, E.A., "Quasi phase matched second harmonic generation by use of a total internal reflection phase shift in gallium arsenide and zinc selenide plates", Optics Letters, 23, 1998, pp. 661-663.

[8] Haidar, R., Forget, N.,Kupecek, P., Rosencher, E.,"Fresnel phase matching for three wave mixing in issotropic semiconductors", Journal of Optical Society of America B, 21, 2004, pp. 1522.

[9] Baudrier-Raybaut, M., Haidar, R., Kupecek, Ph., Lemasson, Ph., Rosencher, E., "Random quasi phase matching in bulk polycrystalline isotropic nonlinear materials", Nature, 432, 2004, pp.374.

[10] Mel'nikov, V.A., Golovan, L.A., Konorov, S.O., Muzychenko, D.A., Fedotov, A.B., Zheltikov, A.M., Timoshenko, V.Yu, and Kashkarov, P.K., "Second harmonic generation in strongly scattering porous gallium phosphide", Applied Physics B, 79, July 2004, pp. 225-228.

[11] Saha, A., and Deb, S., "Broadband second harmonic generation in the near infrared region in a tapered zinc selenide slab using total internal reflection quasi phase matching", Japanese journal of applied physics, 50, 20, October 2011, pp. 102201-1-102201-7.